Imaging artifact precompensation for spatially multiplexed 3-D displays

Joshua Napoli*[a], Sourav R. Dey[b], Sandy Stutsman[a], Oliver S. Cossairt[b], Thomas J. Purtell, II[b], Samuel L. Hill[a], Gregg E. Favalora[a]

[a]Actuality Medical, Inc, 213 Burlington Road, Suite 105, Bedford, MA USA 01730;
[b]Employed by Actuality during performance of this work

PREPRINT

Contact: favalora@actuality-medical.com

         +1 (781) 541-6036 x102

Imaging artifact precompensation for spatially multiplexed 3-D displays

Joshua Napoli*[a], Sourav R. Dey[b], Sandy Stutsman[a], Oliver S. Cossairt[b], Thomas J. Purtell, II[b], Samuel L. Hill[a], Gregg E. Favalora[a]

[a]Actuality Medical, Inc, 213 Burlington Road, Suite 105, Bedford, MA USA 01730;
[b]Employed by Actuality during performance of this work

ABSTRACT

We describe a projection system that presents a 20 megapixel image using a single XGA SLM and time-division multiplexing. The system can be configured as a high-resolution 2-D display or a highly multi-view horizontal parallax display. In this paper, we present a technique for characterizing the light transport function of the display and for precompensating the image for the measured transport function. The techniques can improve the effective quality of the display without modifying its optics. Precompensation is achieved by approximately solving a quadratic optimization problem. Compared to a linear filter, this technique is not limited by a fixed kernel size and can propagate image detail to all related pixels. Large pixel-count images are supported through dividing the problem into blocks. A remedy for blocking artifacts is given. Results of the algorithm are presented based on simulations of a display design. The display characterization method is suitable for experimental designs that may be dim and imperfectly aligned. Simulated results of the characterization and precompensation process are presented. RMS and qualitative improvement of display image quality are demonstrated.

Keywords: high resolution, superresolution, software, autostereoscopic, automultiscopic

1. INTRODUCTION

1.1 Contributions

In this paper, we present methods for characterizing the light transport function of a display and for precompensating the image for that transport function to reduce the effects of optical artifacts, such as defocus. We do this in the context of a development-stage automultiscopic display that is theoretically capable of XGA (1024 x 768) per-view resolution, 24+ views, and 12-bit color depth. The authors cite the work of two key investigators of this effort, Cossairt and Purtell, who designed the display's 20 megapixel image backplane architecture and lenticular array[1,2].

Aspects of this discussion include:

- A *super-resolution* display engine that generates 2-D imagery of at least 25x the resolution as the embedded microdisplay. We report a 5,120 x 3,840 pixel, 12-bit color image produced by a single 1,024 x 768 pixel Texas Instruments (Plano, TX, USA) Digital Micromirror Device (DMD).

- A custom lenticular array that is fabricated to demultiplex a super-resolution image blackplane into the 24-view, XGA-resolution autostereoscopic image

- A method for characterizing the light transport function of the display

- A software-based method for precompensating for the display PSF, to optimize the imagery encumbered by defocus

1.2 Automultiscopic displays

Automultiscopic 3-D displays refer to systems that create the perception of 3-D imagery to the unaided eye by projecting more than two discretized perspective views of a 3-D scene to one or more users. Systems of this nature are also referred to as parallax panoramagrams[3]. The majority of automultiscopic displays project several *views*, visible within several *viewzones*, from a (macroscopically) flat display surface. The display surface typically uses a lenticular lens sheet or

parallax barrier to steer the imagery of a multitude of *subpixels* to the viewzones. Since the subpixels simultaneously encode more than one 2-D image (pertaining to various perspectives), they are usually arranged in an interdigitated, tiled, or other spatially multiplexed pattern. The display surface therefore spatially demultiplexes the subpixels so that they are visible from the appropriate viewzones and, ideally, not in others. Each subpixel of an automultiscopic display modulates or illuminates a particular cone of space in which the major axis is substantially larger than the minor. The *pixel light field* is the distribution of illumination intensity over the relevant programmable dimensions, typically translation along the display image plane and skew around the lenticular axis. The *display light field* is the set of all constituent pixel light fields, and is characterized by the display's *light transport function*.

A variety of automultiscopic displays have been constructed and reported elsewhere. At the time of writing, commercially available automultiscopic displays provide approximately 8-12 views with per-view resolution at or below XGA (1,024 × 768). However, these systems have seen limited commercial success. It is generally recognized that the following characteristics must be improved if they are to find a home within a high-volume application: resolution at or above XGA, 12-bit or higher color depth, >20 views at or above 1 view per degree, and a horizontal field of view that will comfortably accommodate at least one user (e.g. 45 degrees).

Optical physics places fundamental limits on the performance of lenticular sheet displays. Diffraction and geometric-optic aberrations rapidly limit their contrast and brightness. Regardless, there are indications that commercially available displays are not yet up against the limit of "theoretically optimal" display quality. For example, Daniell reported lenticular and fly's-eye lenses that exhibit very high image quality[4]. Several researchers have provided theory describing the limits for the performance of lenticular and integral photography systems[5,6,7]. These publications assume that the image backplane is acquired photographically in a process that passes light through the lens array before striking the emulsion, thus being degraded twice by diffraction and lens aberrations.

The pixel light fields actually produced by autostereoscopic displays are often far from the ideal. The properties of the lenticular array generally cause a great deal of crosstalk. In addition, the set of pixel light fields may be irregular because the axis of the lenticules is normally rotated from the pixel axis to equitably distribute resolution and to reduce moiré patterns[8]. The lenticules are also not typically uniform in structure along each dimension. Jain and Konrad have designed a linear filter for subsampling source images for displays with irregular grids and interview crosstalk[9]. The filter bandlimits the image for the irregular pixel grid to prevent aliasing, though it does not compensate for the crosstalk. Berretty proposes that a high-pass filter be used to reduce crosstalk, but no details on the construction or performance of such a filter are given[10].

Crosstalk in stereoscopic displays can be effectively reduced or canceled by a method proposed by Konrad and Lacotte[11]. They developed a crosstalk cancellation table using a psychcovisual experiment. Each left and right pixel intensity pair is mapped through a table to a new intensity pair that would reduce the perceived crosstalk. This straightforward approach is not practical for multiscopic displays, since the dimensionality of the table would be very high. In a later section, we develop an estimation and pre-compensation technique to reduce crosstalk artifacts.

1.3 High-resolution digital projectors

In this paper, we describe a method for increasing the resolution of projection displays by factors of 2, 4, 9, and up to at least 25× the native resolution of the embedded SLMs. This is desirable for applications such as: projection television, military visualization, digital cinema, and high-performance visualization in the sciences. The resolution of commercially available projection displays is limited by the resolution of the system's SLM, which is often a DMD, D-ILA, or other modulator with resolutions in the range of XGA (1,024 × 768), SXGA (1,280 × 1,024), or HD. Customers desiring a higher-resolution projection display than these standard resolutions must purchase several rear-projection "video cubes" or align the output of multiple projectors onto a single screen. Therefore, a simple opto-electronic module capable of radically increasing the display's resolution is desirable.

This paper refers to the term "super-resolution" as the act of obtaining a higher resolution from a device than its native resolution gives. Super-resolution display methods are duals of methods for high-detail image capture from low-detail input[12]. It may be more appropriate to refer to the technique as "inverse super-resolution."

A technique called "wobulation" was reported by Hewlett-Packard[13,14] that is used in certain rear-projection televisions.

As they explain:

> The basic idea for wobulation was taken from inkjet printing. Resolution of an image is increased when the resolution of the grid on which the pixels are addressed (placed) is increased. This is true, within limits, even if the size of the dots (pixels) is significantly larger than the pitch of the addressed grid. In a wobulated projector, for each frame of image data received, multiple sub-frames of data are generated. Each sub-frame contains unique image information, and is projected onto the screen in a slightly different position by means of an opto-mechanical image shifter. Subframe display is synchronized with the color wheel with at least one full color cycle occurring during the display period of each subframe. This increases the addressed resolution, but does not change the pixel size: pixels from distinct sub-frames overlap. (Allen and Ulichney, pp. 1514-1515)
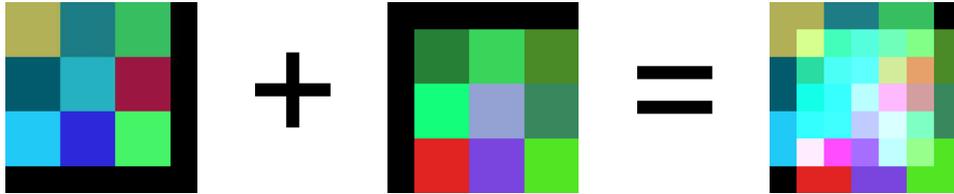

Figure 1: Overlapping sub-frames of pixels that are shifted a fraction of the pixel pitch, as in [13].

A drawback of techniques whose pixel size is greater than the pixel pitch, such as wobulation, is that certain images cannot be reproduced. For example, a high-contrast checkerboard cannot be drawn with a pitch equal to the system's addressable pixel pitch. For that to succeed, the pixel size must match the distance between shifted subframes. We describe a system capable of that in Section 2.

Other methods of increasing the effective addressable resolution of a display have been reported, including those using polarization and birefringence[15,16], pixel-level optical superposition of multiple displays[17], an "optical path changer[18]," and a rotating microprism array[19].

2. SUPER-RESOLUTION DISPLAY

We developed two proof-of-concept super-resolution 2-D display systems that were to act as image backplanes for a highly multi-view 3-D display. They became operational in December, 2005 and March, 2007. Their specifications are as follows:

Table 1: Specifications of two super-resolution display prototypes.

	Mark I (December, 2005)	Mark II (March, 2007)
Embedded light engine	Three DMDs with TIR color prism (1,024 × 768 × 3). "Discovery 1100" chipset. Used off-the-shelf relay and projection optics rather than the ideal prescriptions.	One DLP and 12-segment color wheel with custom neutral-density coatings. "Discovery 3000" LVDS chipset. Used custom illumination, relay, and projection optics.
Super-resolution image resolution	Approx. 5,120 × 3,840 (19.7Mpix)	Approx. 5,120 × 3,840 (19.7Mpix)
Color Depth	1 bit per each of R, G, B	12 bits (4 per R, G, B)

The system described is a projection technology that uses commercially available spatial light modulators. This suggests applications in several areas: (1) rear-projection television, in which DMDs with resolutions that are fractions of HD resolution can be used to provide truly HD resolution, (2) high-resolution desktop or conference-room projection using a single projector rather than ganged, merged imagery, and (3) three-dimensional display.

2.1 Super-resolution theory of operation

Please refer to Figure 2. The Mark I and Mark II super-resolution projectors create 2-D imagery with a resolution that is a multiple (e.g. 2, 4, 9, 25) of the resolution of the embedded microdisplay. They trade off the excess frame rate of the TI DMD to yield additional pixels. Importantly, the resulting pixels abut each other; they do not overlap. This provides a truly higher-resolution image capable of representing high-frequency information with a higher dynamic range than techniques like wobulation.
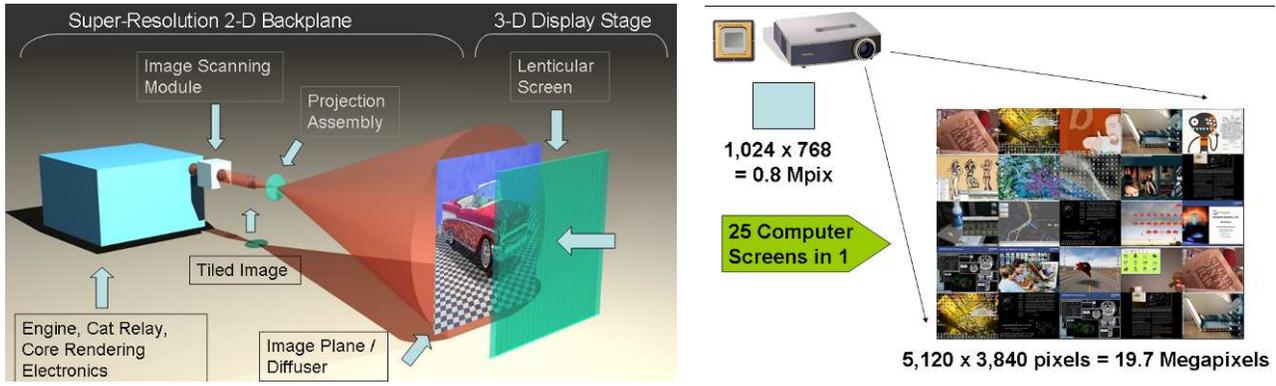
Figure 2: (Left) A super-resolution projector can act as the backplane for a high-resolution 25-view automultiscopic display. (Right) The SR projector can create 19.7 Mpix imagery from a single 0.8 Mpix DMD.

This occurs in a multi-step process. We describe this in terms of the Mark II system. First, a desired 5,120 × 3,840 image in the PNG format is loaded into a software application that re-orders the pixels into (25 XGA-resolution DMD frames of SR subpixels × 12 color bits/frame) = 300 single-color DMD frames. These frames are modified to precompensate for optical imperfections by an algorithm described later in this paper, and are resampled to match its sheared display coordinate system. The frames are loaded into a DMD controller board/frame buffer capable of 13 kHz replay (ALP-3, ViALUX Messtechnik + Bildverarbeitung GmbH, Chemnitz, Germany). The high-speed playback is synchronized to the color wheel's phase and scan angle of a piezoelectric mirror scanner (Piezosystem Jena,GmbH, Jena, Germany).

The system's optical path is shown in Figure 3. A dual-paraboloid reflector (Wavien, Inc, Valencia, CA) and 150 W lamp illuminate an XGA-resolution "Discovery 3000" DMD board (DLi, Austin, TX). The image of the DMD is re-imaged to a physically-accessible location (the *intermediate image plane*) by a custom catadioptric 1:1 relay. An aperture array (Heptagon, Rueschlikon, Switzerland) with an active area equal to that of the XGA DMD intermediate image is located at the intermediate image plane. In the case of our 25× system, the aperture array is tiled by a periodic square array of pitch matching the DMD pixels (13.68 um on a side). Each square "unit cell" contains a transparent region of 1/25 the area of the unit cell.

The aperture array thus creates a point-like grid of spaced-apart super-resolution subpixels, as shown in Figure 4 and Figure 6. While the DMD repeatedly projects the sequence of 300 frames, the single-axis piezoelectric scanner sweeps the subpixel grid at an angle that satisfies the condition that after 25 time steps all subpixels form a continuous grid of subpixels, which abut and do not overlap. The 25-step process repeats 12 times, once for each segment of the rotating color wheel. This is illustrated in Figure 5 as four example time steps and the resulting image.

Therefore, the system can depict images with pixel sizes that are a fraction of the native DMD pixel image size. This occurs when the area and pattern of the apertures at the intermediate image plane is properly matched to the desired resolution multiplication factor and the orientation of the scanner's scan axis. A particular scan angle and scan sweep distance will allow the light passing through a tiling of apertures to "meet up." In Mark II, for example, the piezo scanner was configured to provide scanlines at a tilt of approximately 11° (= atan(5/25)) in the final (i.e. projected) image plane. The piezo scanned at 5 mrad (0.3°) at approximately 30 Hz. In Mark I, the scan was 2-D and boustrophedonic; in Mark II, it was 1-D and tilted. This simplified the optical design because only one scanner was needed, and it operated at low frequency.
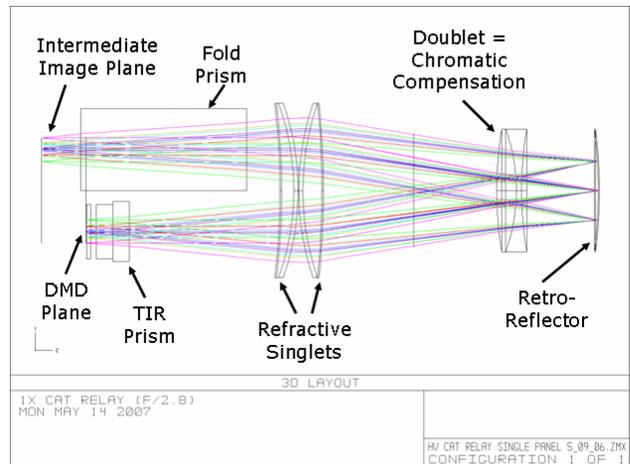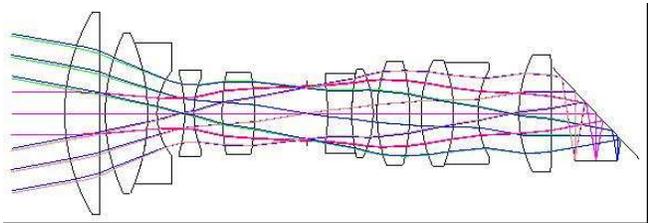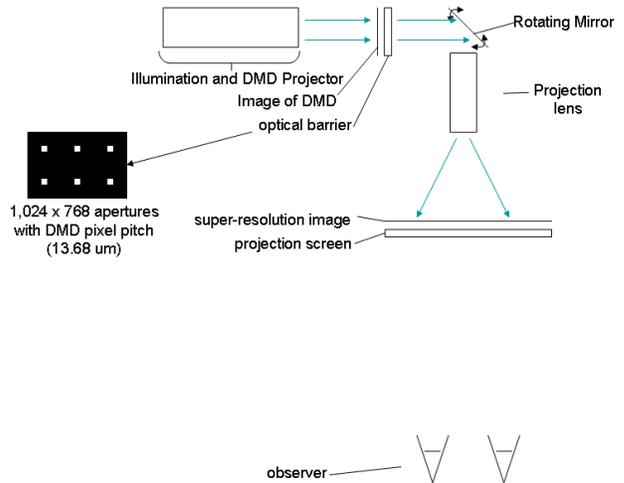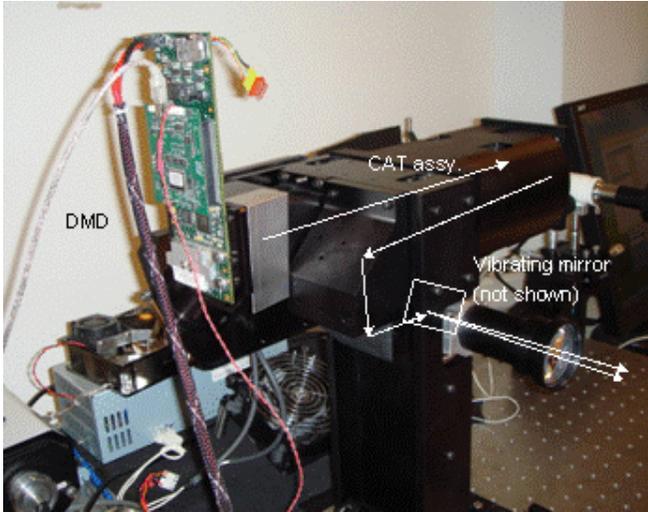
Figure 3: (Clockwise from upper left.) Mark II SR. Simplified schematic optical path; a series of 300 XGA-resolution images are windowed by an aperture array and scanned at an angle and pitch that creates a contiguous pixel grid after 25 time steps. CAT 1:1 relay. Custom projection lens assembly.
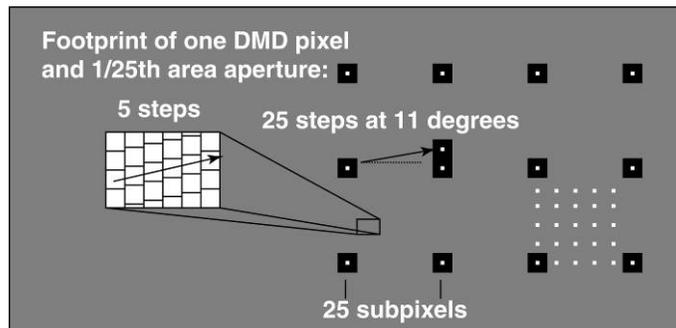

Figure 4: 5-by-5 (25x) super-resolution scans the image of the aperture array at 11.3° (= atan (5/25)) above horizontal in a sequence of 25 time steps. Illuminating every DMD pixel for only one time step creates a field of subpixels spaced 5 apart in each direction (white squares, lower right). The coordinate system is sheared vertically. Every deflected sub-pixel moves vertically the length of one sub-pixel every 5 time steps, which matches vertically the height of a DMD pixel image every 25 time steps. One time instant is illustrated here, in which sub-pixels are white and the windowed DMD pixel footprints are black. For clarity, they are drawn spaced 5 DMD pixels apart.
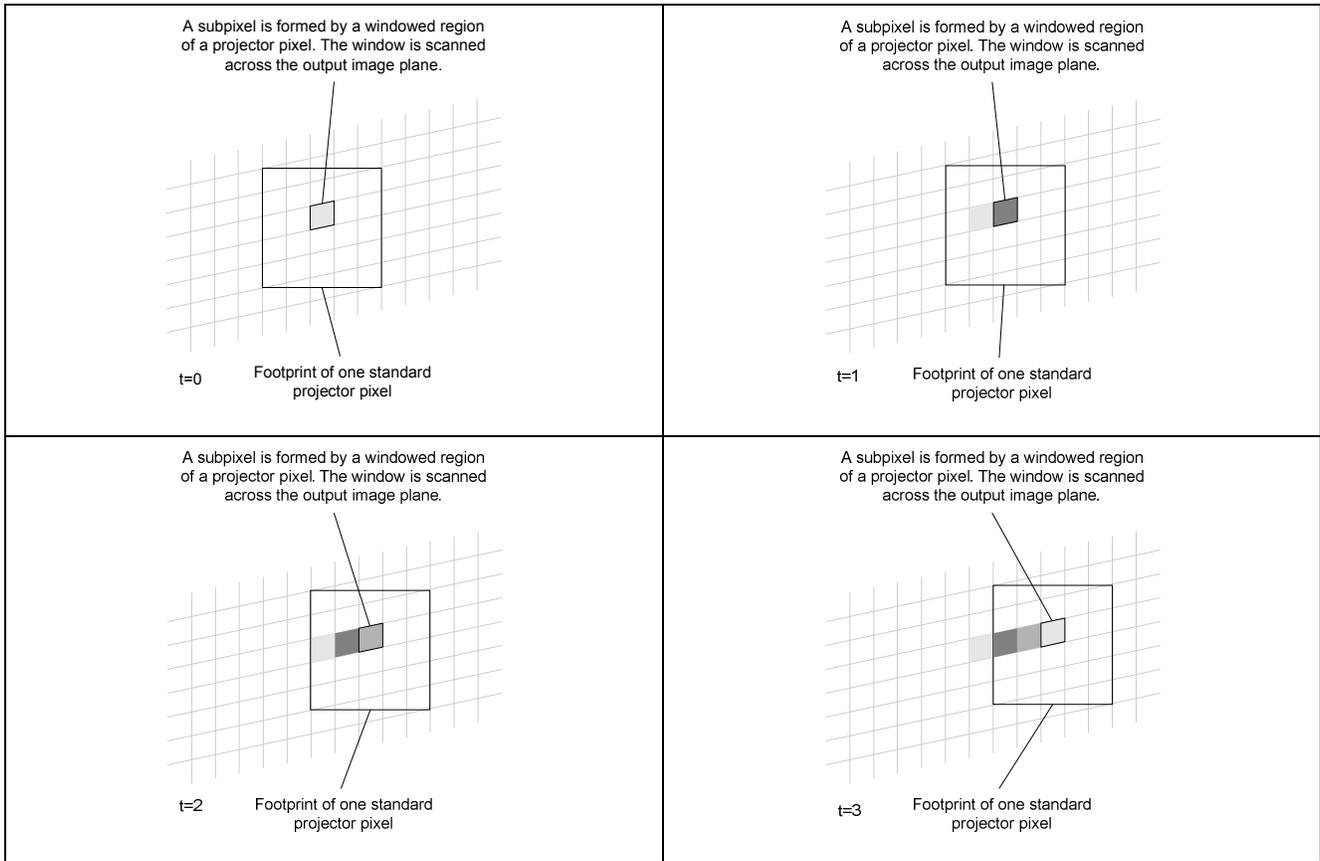
Figure 5: (Read in scanline order.) Our super-resolution image projection process scans fractional DMD pixels along an angle that is matched to the resolution multiplication factor so that resulting pixels abut. This generates an image that is higher-resolution in terms of addressable pixels and the spatial frequency content of the imagery. The figure shows four subpixels being formed as the windowed DMD pixel scans across the output image.

2.2 Results

The system successfully projected a variety of images with the specifications noted above. A test image from the system is provided on the right side of Figure 6. This 20 Mpix image was assessed in rear-projection at a diagonal of 18" (46 cm) and front-projection with a diagonal of 60" (152 cm). This corresponds to a subpixel pitch of 71 μm and 238 μm, respectively.

However, the Mark II prototype exhibited significant defocus. Extensive examination of the issue suggested it was caused by the 1:1 CAT relay. Because of this, the light reflected by each DMD pixel was projected onto a field of many apertures rather than just one. This caused crosstalk in the final super-resolution image, in that a 2-D collection of pixels 5 subpixels apart were correlated. This decreased the contrast of the image, and ultimately hampered the creation of a 3-D image. It motivates the development of the precompensation algorithms described in the next section.

3. CHARACTERIZATION OF A 3-D DISPLAY LIGHT FIELD

3.1 Automultiscopic operation and custom lenticular array

For the automultiscopic configuration of the Mark II display engine, a custom lenticular array was designed and fabricated (Anteryon, Eindhoven, The Netherlands) to convert the 20 Mpix 2-D image into a 25-view, XGA-resolution 3-D image. To achieve this goal, we designed the lens with sufficient MTF for 32 views at 40 lpmm. We used a biconvex lens array sandwiched between two thin glass substrates, as shown in Figure 8.
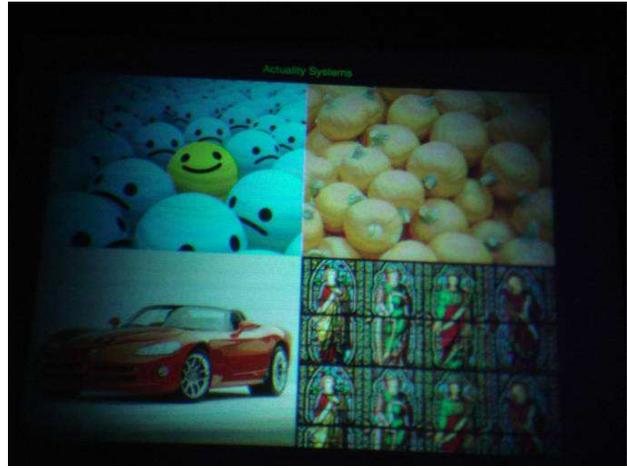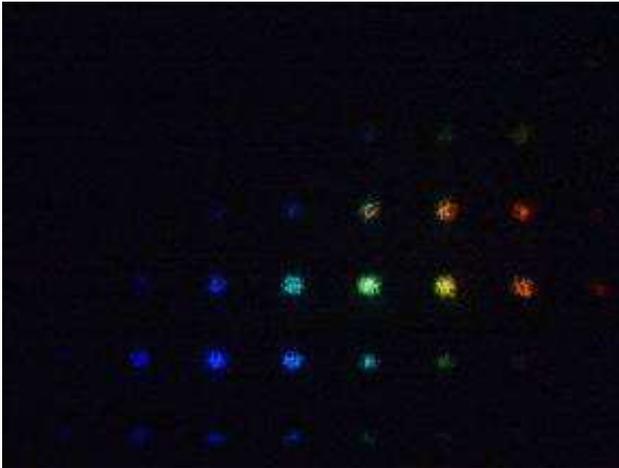
Figure 6: (Left) Photograph of an instantaneous field of multiple subpixels taken with the piezo scanner deactivated and a single DMD pixel lit. Ideally, a single subpixel would be visible. This crosstalk is likely due to the design, manufacture, or alignment of the CAT relay in the prototype. (Right) 20 megapixel image.
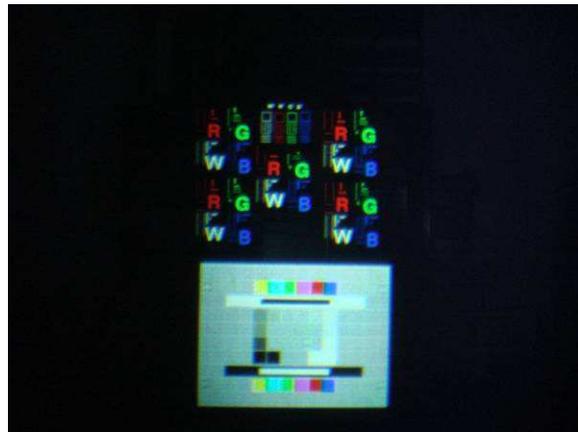

Figure 7: (Left) An upconverted XGA image depicted in the foreground in the desktop SR display and in the background on an LCD display. (Right) Cropped photograph showing 2/25 of the area of the SR system showing a region with (1,024 × 1,536) pixels within an approximately 3" wide region.
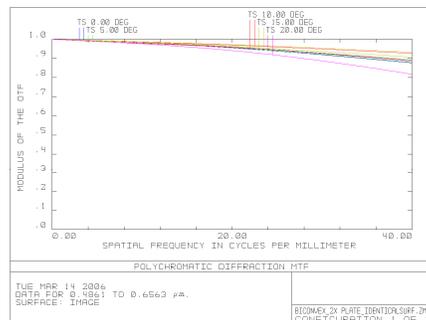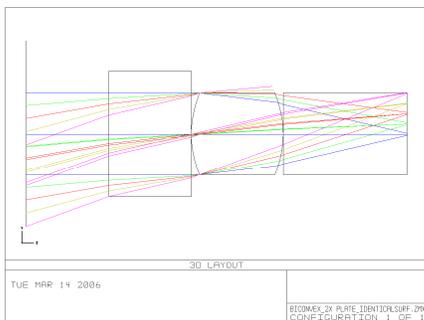

Figure 8: The lenticular screen design consists of a biconvex lenticular lens sandwiched by two thin glass substrates. The MTF of these lenses (shown on the right) is near diffraction-limited for providing 32 views at 40 lpmm.

As noted in Section 2.2, the sub-pixel pitch at the lenticular is 71 μm, operating in rear-projection mode. Particular care must be taken to compute the input imagery so that they are relayed to the appropriate viewing zones, since small offsets or angulations of the screen with respect to the 3-D rendering software's assumptions can create artifacts. Therefore, we developed a method to fully characterize the system's light field.

3.2 Display characterization

For the automultiscopic configuration of the Mark II display engine, software was developed to resample a multiscopic source image for the display using a detailed measurement of the light transport function. A characterization procedure for the display was developed. A similar procedure may be of use with other lenticular displays where there is some mismatch between the placement of lenticular sheet and the pixel array.

To calibrate our display, a grayscale Sony XCD-SX910 camera was used. The distance from the camera to the display was set such that there would be at least one camera pixel for each display pixel. Our calibration software used OpenCV to calibrate the camera with its lens. The software also used OpenCV to detect fiducial markers at the corners of the frame of our display. The corner fiducials allowed the software to calculate the precise position of the camera and to warp and crop each frame so that the active display area would be rectangular 1024×768 image. The calibration software programmed the display to present a sequence of pseudorandom calibration images. To reduce ambiguity, the calibration images were constructed such that source pixels that would likely result in overlapping camera images would not be simultaneously lit. The sequence of calibration images was recorded from enough poses to sample the entire display light field.

The resampling software for the Mark II display is designed to interpret the calibration data by determining a minimum and maximum bound on the possible contribution to each camera pixel of a given display subpixel. To reduce the size of the resulting data structure, it is assumed that a display subpixel will only affect the 3x3 block of camera pixels determined by the designed ray-trace. No assumption is made about which views are affected by each display pixel. The process defines a set of calibration pairs $\{ (D_i, C_{i,j}) \}$ of binary driving functions, D_i, and a camera image, $C_{i,j}$, in each pose j. The calibration process also measures the maximum (all pixels on) light output of the display for each view, I_j.

The set of calibration pairs is used to estimate F, the light transport function. Consider a single pixel light field, corresponding to display pixel (x,y). Let $A_{x,y}$ be the set of calibration image indexes such that the pixel (x,y) is illuminated and $\overline{A_{x,y}}$ the set where the pixel is not illuminated. We can use A to establish an upper bound on the contribution to camera pixel intensity levels from the display pixel (x,y). Let $C_{i,j,s,t}$ be the value of pixel (s,t) of camera j. For pixel (s,t) of camera j, the maximum contribution from display pixel (x,y) is the minimum of the camera image values, $C_{i,j,s,t}$, over the calibration images indexed by $A_{x,y}$. $\overline{A_{x,y}}$ establishes a lower bound on the camera pixel intensity levels. The minimum possible contribution to camera pixel (s,t) from display pixel (x,y) is the maximum of $I_j - C_{i,j,s,t}$ over the calibration images indexed by $\overline{A_{x,y}}$. Therefore, the light transport coefficient $F_{x,y,j,s,t}$ from display pixel (x,y) to pixel (s,t) of camera j is

$$\max_{i \in A_{x,y}, \ \forall j} \left(I_j - C_{i,j,s,t} \right) \le F_{x,y,j,s,t} \le \min_{i \in A_{j,x,y}, \ \forall j} \left(C_{i,j,s,t} \right) \tag{1}$$

Additional calibration pairs can be acquired until the bounds are tight enough.

4. PRECOMPENSATION

We wish to create an image, P^*, that is *precompensated* for the particular light transport function of a display, F, so that the result comes as close as possible to the desired source image I. The problem can be posed as a constrained minimization.

$$P^* = \min_P \left(\| F \cdot P - I \| \right) \tag{2}$$

To solve for P^*, we used a gradient descent technique that Sen demonstrated to work well for the case of projector blur due to an uneven projection surface[20]. An overview of other optimization techniques for a similar debluring task with wobulation displays is given by Said[21]. The following equations describe the gradient descent algorithm that we used.

P_i is the i-th estimate of P^* produced by the algorithm. We initialize with $P_0 = I$. G is the error gradient.

$$G_i = F^T \cdot \left(I - F \cdot P_i \right) \tag{3}$$

The step scale factor is η.

$$\eta_i = \frac{\left\| G_i \right\|^2}{\left\| F \cdot G_i \right\|^2} \tag{3}$$

$\widetilde{P}$ is the result of stepping along the error gradient direction from the previous estimate of P^*.

$$\widetilde{P}_i = P_{i-1} + \eta_{i-1} G_{i-1} \tag{4}$$

The next estimate of P^* is formed by clamping $\widetilde{P}$ to the dynamic range of the display.

$$P_i = \text{Clamp}\left(\widetilde{P}_i \right) \tag{5}$$

With large images, it can be convenient to break the optimization problem down into parts, so that the precompensation algorithm can iterate without cache misses. To do this, the display's pixels are partitioned into blocks that correspond to small regions of the desired image. However, unless special attention is paid to the borders of blocks, new artifacts are introduced. To eliminate these artifacts, the desired image regions can be arranged to have overlapping borders. In the precompensation algorithm, the borders should be "feathered" by scaling the desired image pixel values with a mask. For a pixel of the desired image that is mapped to more than one block, the mask effectively allocates the responsibility of producing the energy of the pixel to the different blocks. One way to define the mask values for a block is by using the display's light transport function to determine the portion of the total illumination that a desired image pixel would receive from the block when all display pixels are fully activated. In any case, the sum of the mask values of each desired image pixel over all blocks must equal one.
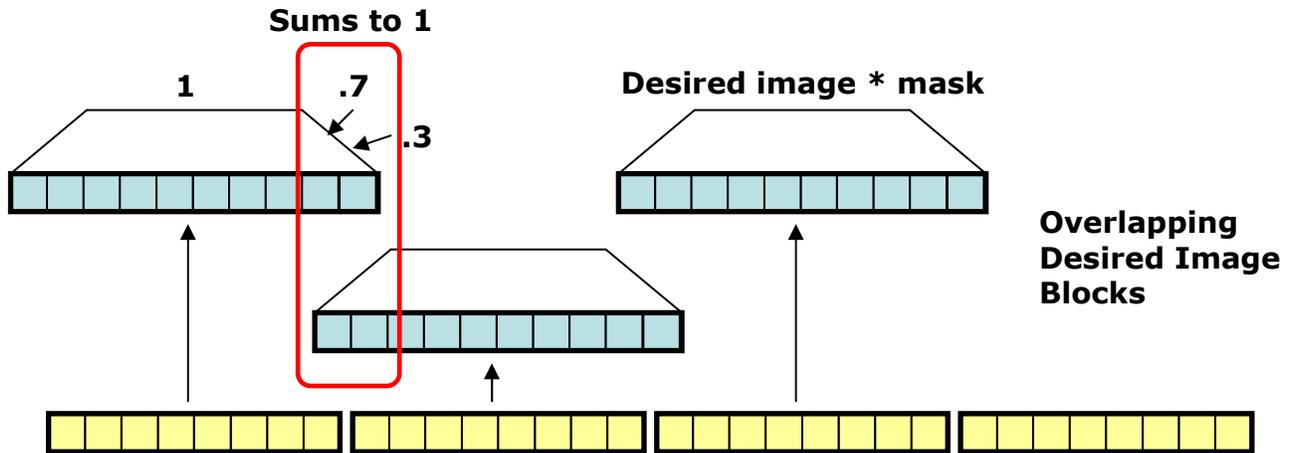

Figure 9: Illustration of processing a source image (represented at the bottom of the figure) being constructed from overlapping blocks (represented at the top of the figure). Precompensation is applied block-by-block. To avoid a blocking artifact, blocks must overlap. A mask scales the desired image values.

5. SIMULATION RESULTS

Simulated results of the characterization process are presented. In the test case shown in Figure 10, a typical multiview display is simulated with relatively severe crosstalk. 50% of the output intensity comes from the central subpixel of the view zone, with the remainder coming from two neighboring subpixels. Three cropped views are shown from the perspective of a monoscopic observer. In the naïve case, the raw source image is directly imaged by the simulated display with crosstalk. In the precompensated case, the result of the crosstalk simulation applied to the result of the gradient descent algorithm is shown. RMS pixel intensity error was reduced from 22 to 13 (in units of maximum intensity).

Figure 10: A selection of monoscopic views of a simulated multiscopic display comparing crosstalk precompensation

One issue observed is limited dynamic range. We illustrate this issue with an example. The next two figures show a simulation of a 2-D super-resolution display. Once again, the effect of the display's light transport function on an unprocessed image (naïve) is compared with the precompensated image. The simulation uses a discontinuous point spread function, based on the pixel replication artifact observed in the Mark II display. The artifact causes a discontinuous point spread function. Pixel replication blends image values separated by small distances in the image, and so there are much larger errors. Because of this, there is insufficient dynamic range and most of the precompensation image pixels are saturated (Figure 11). Note that error from the image edge is propagated across the precompensation image. Nevertheless, the result shown in Figure 12 appears substantially improved, compared to the naïve rendering.
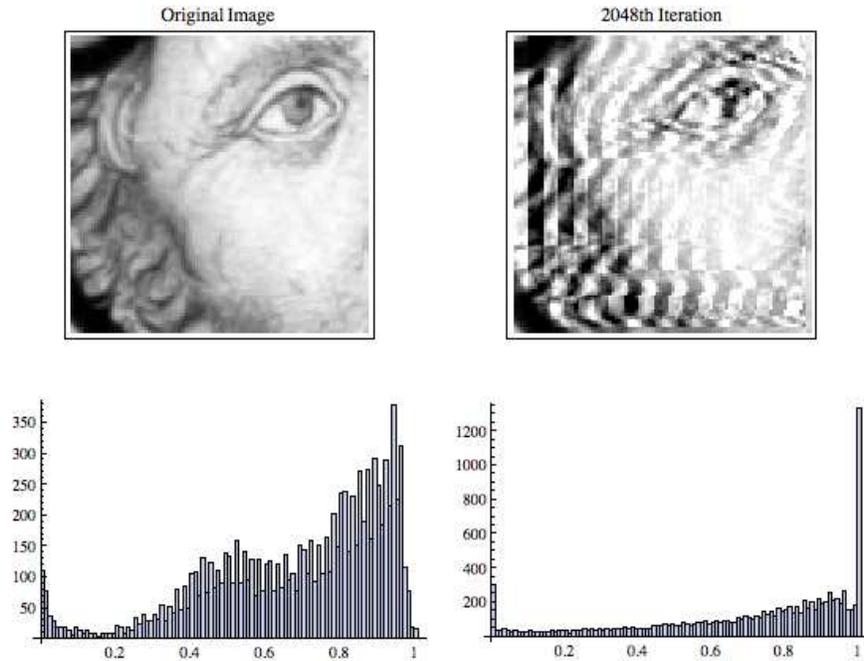

Figure 11: The upper-right image shows the raw precompensated image. The lower charts show that most of the precompensated pixels have saturated, due to insufficient dynamic range.
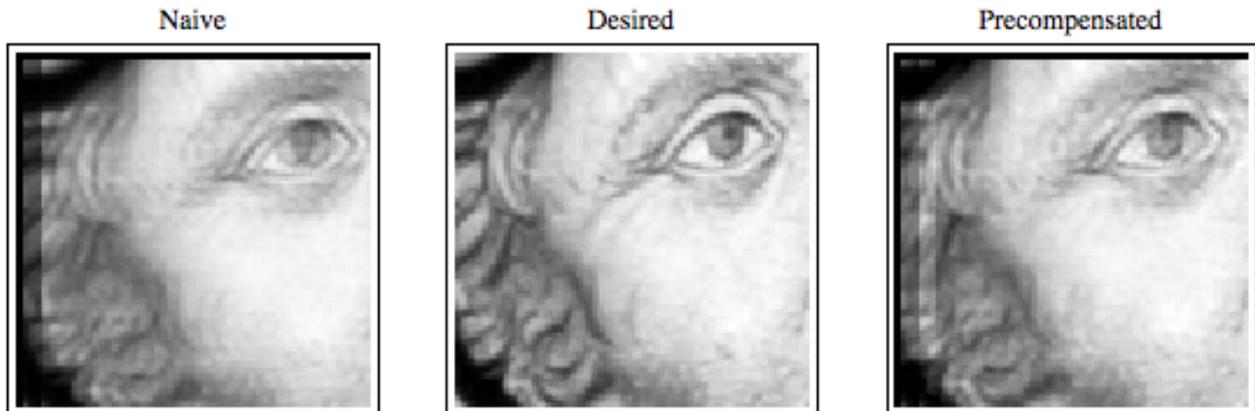

Figure 12: Comparison of precompensated image for a 2-D display with a pixel replication artifact.

ACKNOWLEDGEMENTS

REFERENCES

[1] O. S. Cossairt, T. J. Purtell, II, S. L. Hill, "Optically enhanced image sequences," U.S. Pat. App. Serial No. 11/614,548 (Filed 21 Dec. 2006, claiming priority of U.S. Provisional Nos. 60/791,277 filed 11 Apr. 2006 and 60/752,316 filed 21 Dec. 2005).

[2] O. Cossairt, "Image enhancement for three-dimensional displays," U.S. Pat. Pub. No. 2007-0201133 A1 (30 Aug. 2007).

[3] M. Halle, "Autostereoscopic displays and computer graphics," Computer Graphics, ACM SIGGRAPH 31(2), 58-62 (May 1997).

[4] S. Daniell, "Correction of aberrations in lens-based 3D displays," in Stereoscopic Displays and Virtual Reality Systems XII, edited by Andrew J. Woods, Mark T. Bolas, John O. Merritt, Ian E. McDowall, Proceedings of SPIE-IS&T Electronic Imaging, SPIE Vol. 5664, 175-185 (2005).

[5] C. R. Burckhardt, "Optimum Parameters and Resolution Limitation of Integral Photography," J. Opt. Soc. Am., 58(1), 71-76 (Jan. 1968).

[6] T. Okoshi, "Optimum Design and Depth Resolution of Lens-Sheet and Projection-Type Three-Dimensional Displays," Applied Optics, 10(10), 2284-2291 (Oct. 1971).

[7] H. Hoshino, F. Okano, H. Isono, and I. Yuyama, "Analysis of resolution limitation of integral photography," J. Opt. Soc. Am. A, 15(6), 2059-2065 (Aug. 1998).

[8] D. Winnek, "Composite stereography," U.S. Pat. 3,409,351 (Nov. 1968).

[9] A. Jain and J. Konrad, "Crosstalk in automultiscopic 3-D displays: Blessing in disguise?" in *Stereoscopic Displays and Virtual Reality Systems XIV,* edited by Andrew J. Woods, Neil A. Dodgson, John O. Merritt, Mark T. Bolas, Ian E. McDowall, Proceedings of SPIE-IS&T Electronic Imaging, SPIE Vol. **6490**, 649012 (2007)

[10] R. Berretty, "Rendering of Image Data for Multi-view Display," International patent application, WO/2007/052216

[11] J. Konrad, B. Lacotte, and E. Dubois, "Cancellation of image crosstalk in time-sequential displays of stereoscopic video," IEEE Trans. on Image Processing, 9(5), 897-908 (May 2000).

[12] S. C. Park, M. K. Park, M. G. Kang, "Super-Resolution Image Reconstruction: A Technical Overview," IEEE Signal Processing Magazine, 21-36 (May 2003).

[13] W. Allen and R. Ulichney, "Wobulation: Doubling the Address Resolution of Projection Displays," SID 05 Digest, 1514-1517 (2005).

[14] M. A. Pate, W. J. Allen, M. D. Long, P. G. Howard, and J. M. Koegler, III, "Image display system and method," U.S. Pat. 6,963,319 (8 Nov. 2005).

[15] J. L. Fergason, "Optical display system and method, active and passive dithering using birefringence, color image superpositioning and display enhancement," U.S. Pat. 6,184,969 (6 Feb. 2001).

[16] H. Hiroyuki, "Projection display device," EPO / Japanese patent publication 04113308 (14-04-92).

[17] C. Ciacci, A. P. Cavallerano, "Method and apparatus for increasing the spatial resolution of a projected pixilated display," U.S. Pat. 6,575,576 (10 Jun. 2003).

[18] Y. Shirochi, "Display for mosaic pattern of pixel information with optical pixel shift for high resolution," U.S. Pat. 5,689,283 (18 Nov. 1997).

[19] K.-H. Cho, D.-S. Kim, S.-H. Kim, H.-J. Lee, and T.-H. Kim, "High-resolution display including pixel moving optical system," European Patent Application pub. no. EP 1 387 205 A1 (04.02.2004).

[20] L. Zhang, and S. Nayar, "Projection Defocus Analysis for Scene Capture and Image Display," SIGGRAPH 2006 Conference Proceedings, 907—915

[21] A. Said, "Analysis of Systems for Superimposing Projected Images," HP Tech. Rep. HPL-2006-129 (Oct. 5, 2006).